chemengineering

MDPI

Supplementary Materials

CNT and H_2 Production during CH_4 Decomposition over Ni/$CeZrO_2$. II. Catalyst Performance and its Regeneration in a Fluidized Bed

Agata Łamacz [1,*] and Grzegorz Łabojko [2]

[1] Division of Chemistry and Technology of Fuels, Wroclaw University of Technology, Gdanska 7/9, 50-344 Wroclaw, Poland
[2] Institute for Chemical Processing of Coal, Zamkowa 1, 41-803 Zabrze, Poland. glabojko@ichpw.pl
* Correspondence: agata.lamacz@pwr.edu.pl

Received: 18 January 2019; Accepted: 14 February 2019; Published: date

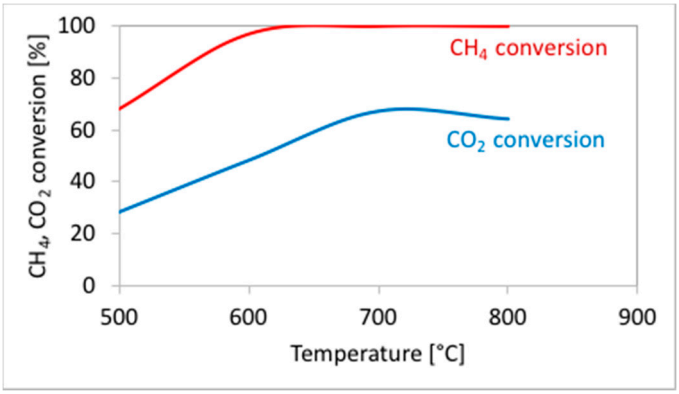

Figure S1. CH_4 and CO_2 conversion during dry reforming of methane over Ni/$CeZrO_2$@CNT hybrid catalyst.

Table S1. Mass increase of Ni/$CeZrO_2$ (0.125–0.2 mm) after tests of CH_4 decomposition at various T, t and GHSV.

Sample	T (°C)	t (h)	GHSV (h^{-1})	Δm (%)
A6/1_5	600	1	5 000	7
A6/3_5	600	3	5 000	11
A6/5_5	600	5	5 000	17
A6/1_10	600	1	10 000	8
A6/3_10	600	3	10 000	10
A6/5_10	600	5	10 000	13
A6/1_20	600	1	20 000	4
A6/3_20	600	3	20 000	7
A6/5_20	600	5	20 000	9
A7/1_5	700	1	5 000	18
A7/3_5	700	3	5 000	43
A7/5_5	700	5	5 000	51
A7/1_10	700	1	10 000	13
A7/3_10	700	3	10 000	37
A7/5_10	700	5	10 000	41
A7/1_20	700	1	20 000	12
A7/3_20	700	3	20 000	29
A7/5_20	700	5	20 000	33

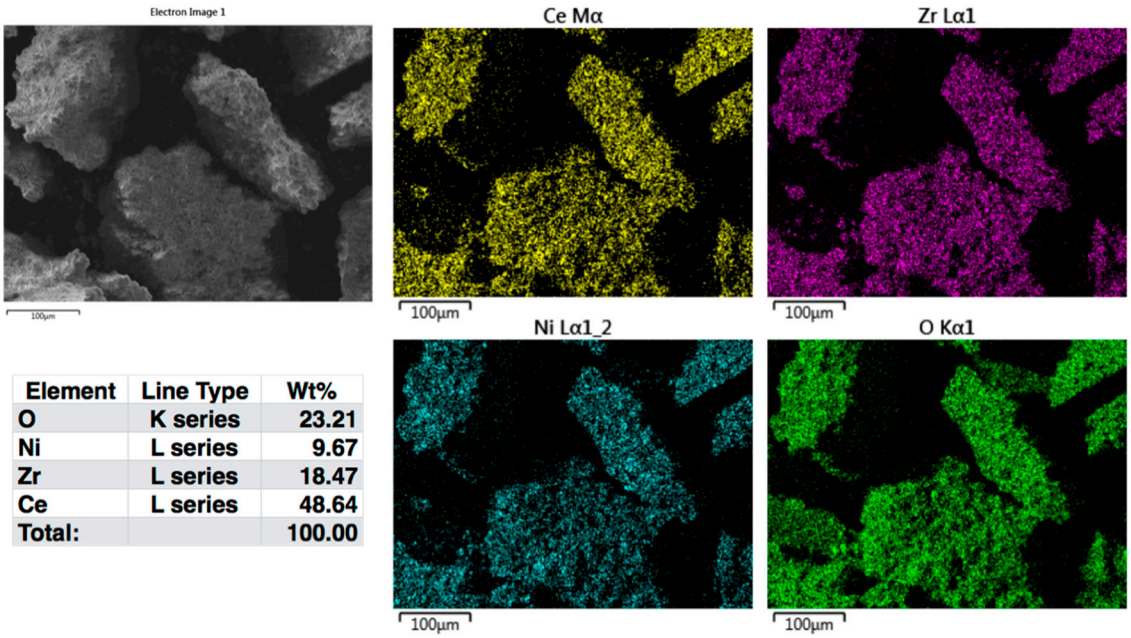

Element	Line Type	Wt%
O	K series	23.21
Ni	L series	9.67
Zr	L series	18.47
Ce	L series	48.64
Total:		100.00

Figure S2. SEM picture, Ni, Ce, Zr and O mapping and composition of Ni/CeZrO$_2$ before CH$_4$ decomposition.

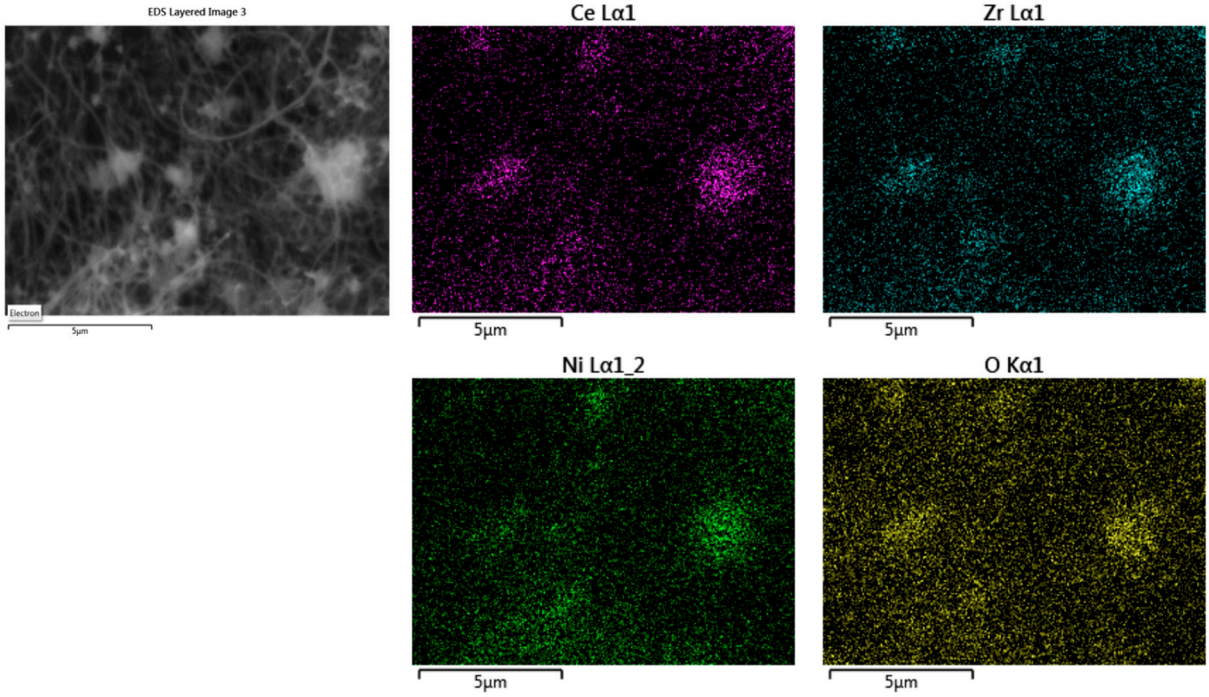

Figure S3. SEM picture, Ni, Ce, Zr and O mapping for Ni/CeZrO$_2$ after CH$_4$ decomposition (700 °C/5 h, GHSV = 10,000 h^{-1}).

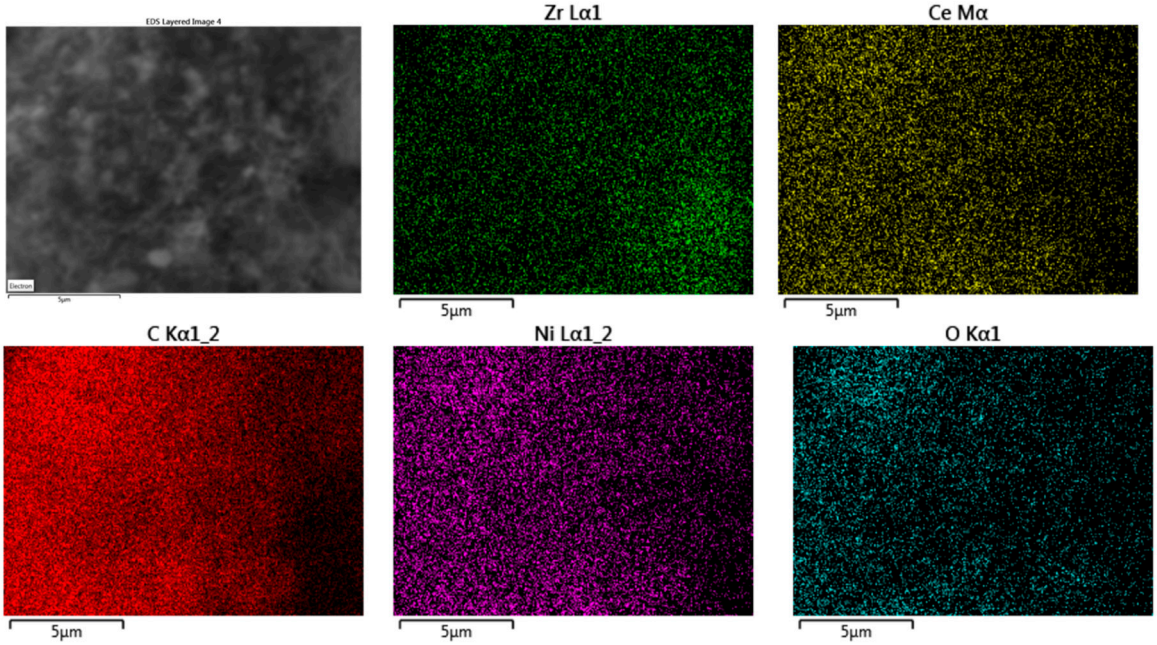

Figure S4. SEM picture, Ni, Ce, Zr and O mapping for Ni/CeZrO2 after separation of carbon deposit.

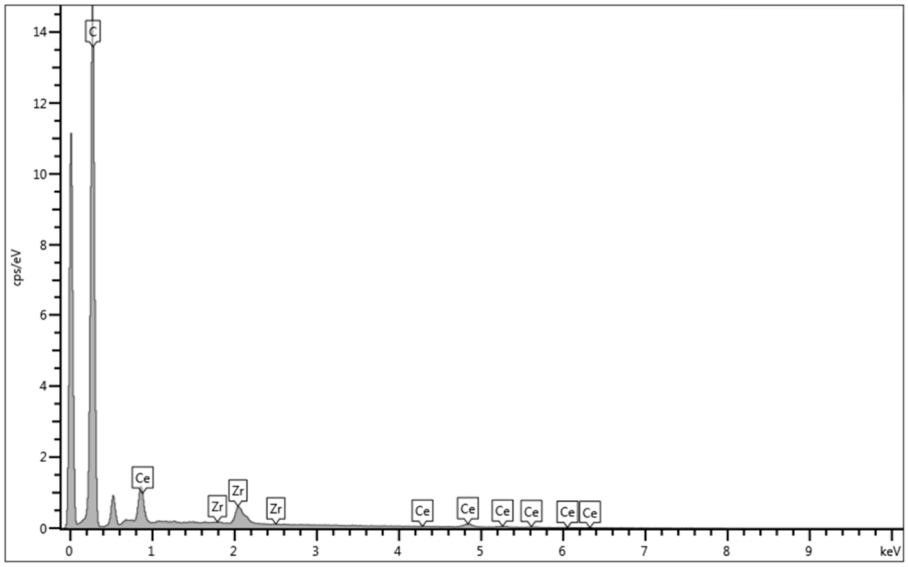

Figure S5. EDS spectra for carbon fraction after separation from Ni/CeZrO2.

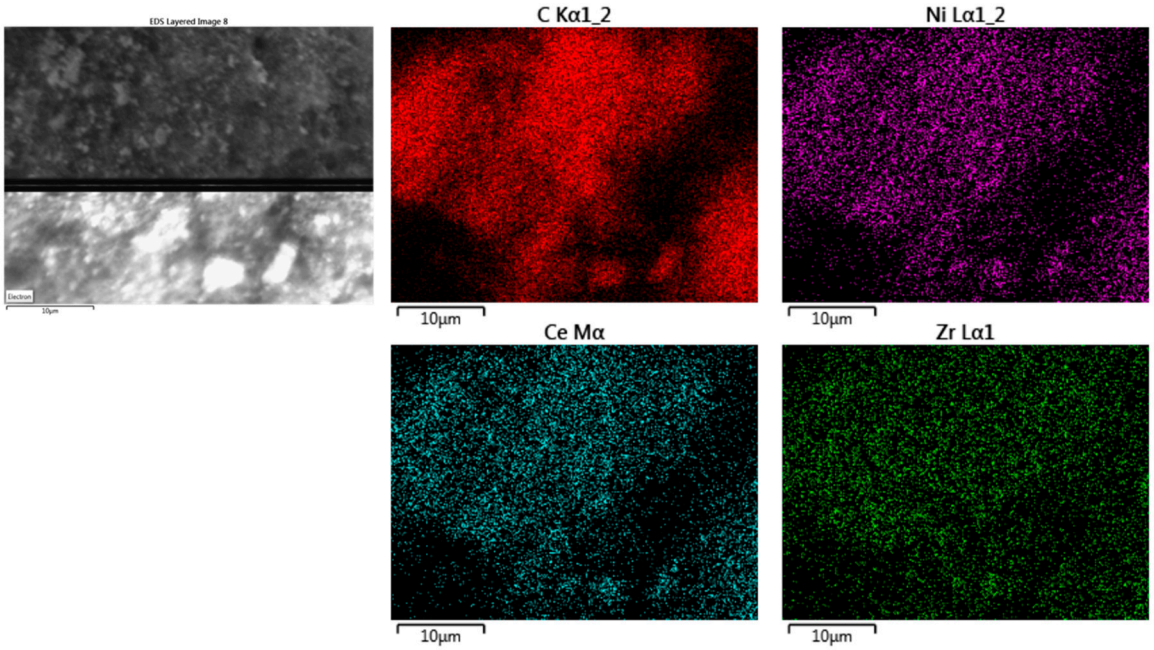

Figure S6. SEM picture and Ni, Ce, Zr and O mapping for carbon fraction after separation from Ni/$CeZrO_2$.

Table S2. Mass increase of Ni-MgO after tests of CH_4 decomposition at various T, t and GHSV.

Sample	T (°C)	t (h)	GHSV (h^{-1})	Δm (%)
B6/1_10	600	1	10,000	26
B6/3_10	600	3	10,000	44
B6/5_10	600	5	10,000	51
B6/1_20	600	1	20,000	24
B6/3_20	600	3	20,000	40
B6/5_20	600	5	20,000	43
B7/1_10	700	1	10,000	63
B7/3_10	700	3	10,000	76
B7/5_10	700	5	10,000	80
B7/1_20	700	1	20,000	55
B7/3_20	700	3	20,000	60
B7/5_20	700	5	20,000	62

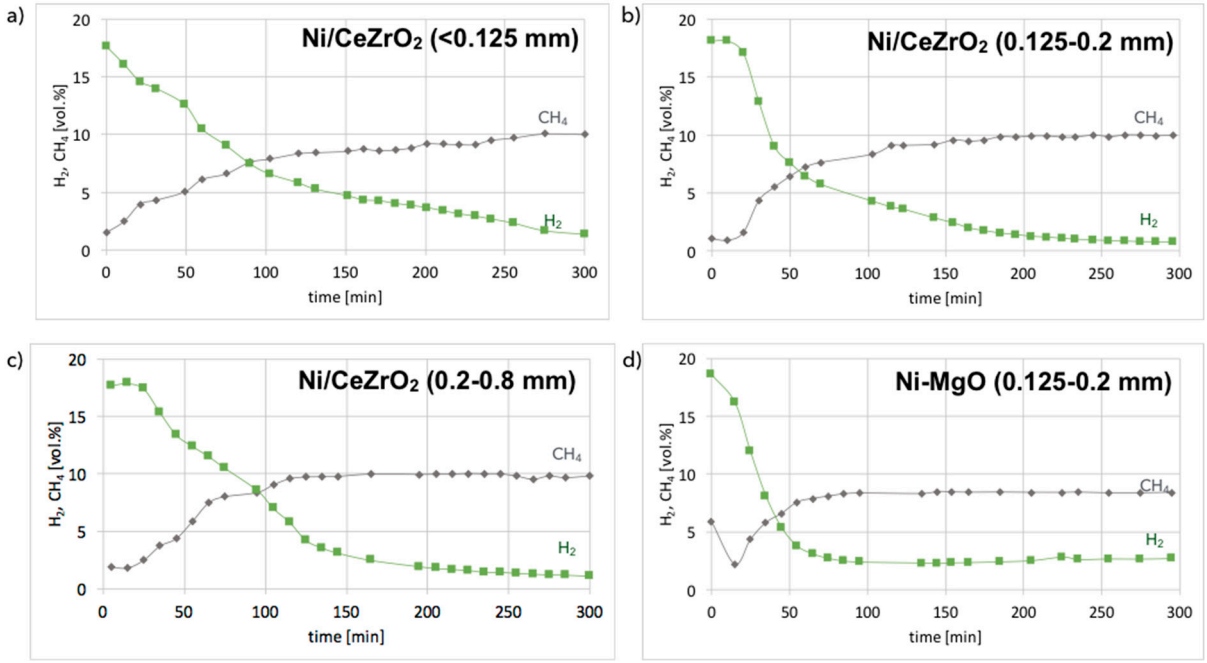

Figure S7. Composition of the outlet gas from fluidized bed reactor during CH_4 decomposition on $Ni/CeZrO_2$ and Ni/MgO catalysts (T = 700 °C; GHSV = 10,000 h^{-1}).

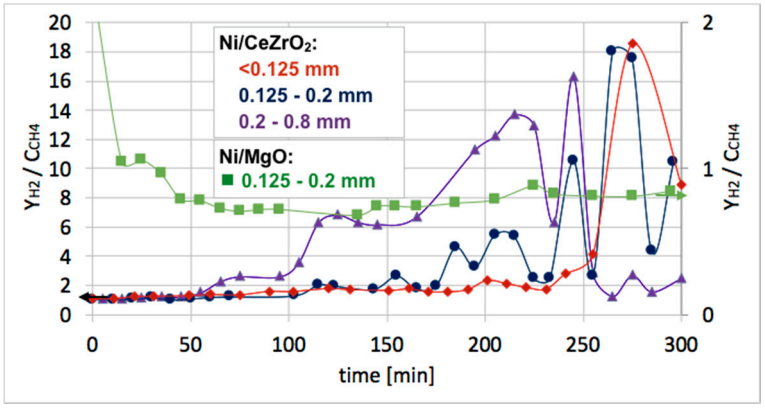

Figure S8. CH_4 conversion to H_2 yield (C_{CH_4}/Y_{H_2}) ratio during CH_4 decomposition on $Ni/CeZrO_2$ and Ni/MgO catalysts (T = 700 °C; GHSV = 10,000 h^{-1}).

Table S3. CH_4 consumption and H_2 production per 1 mol of Ni in $Ni/CeZrO_2$ and Ni-MgO during CH_4 decomposition tests.

$Ni/CeZrO_2$	CH_4/Ni (mol/mol)	H_2/Ni (mol/mol)
1st	12.36	24.44
2nd	10.56	18.55
3rd	8.51	12.11
4th	5.50	9.60
NiMgO	2.29	3.88

Regeneration of $Ni/CeZrO_2$ in H_2O in Temperature Programmed Conditions in Micro-Reactor.

Regeneration of $Ni/CeZrO_2$ was carried out in flowing 4.15 vol.% H_2O/Ar under GHSV of 5000 h^{-1}. The samples used for regeneration were obtained after CH_4 decomposition at 700 °C carried out for 1, 3 and 5 h in GHSV of 5000 and 20,000 h^{-1}. Yields of H_2, CO and CO_2 as a function of temperature during regeneration tests are presented in Figure S9. Conversion of H_2O is shown in Figure S10.

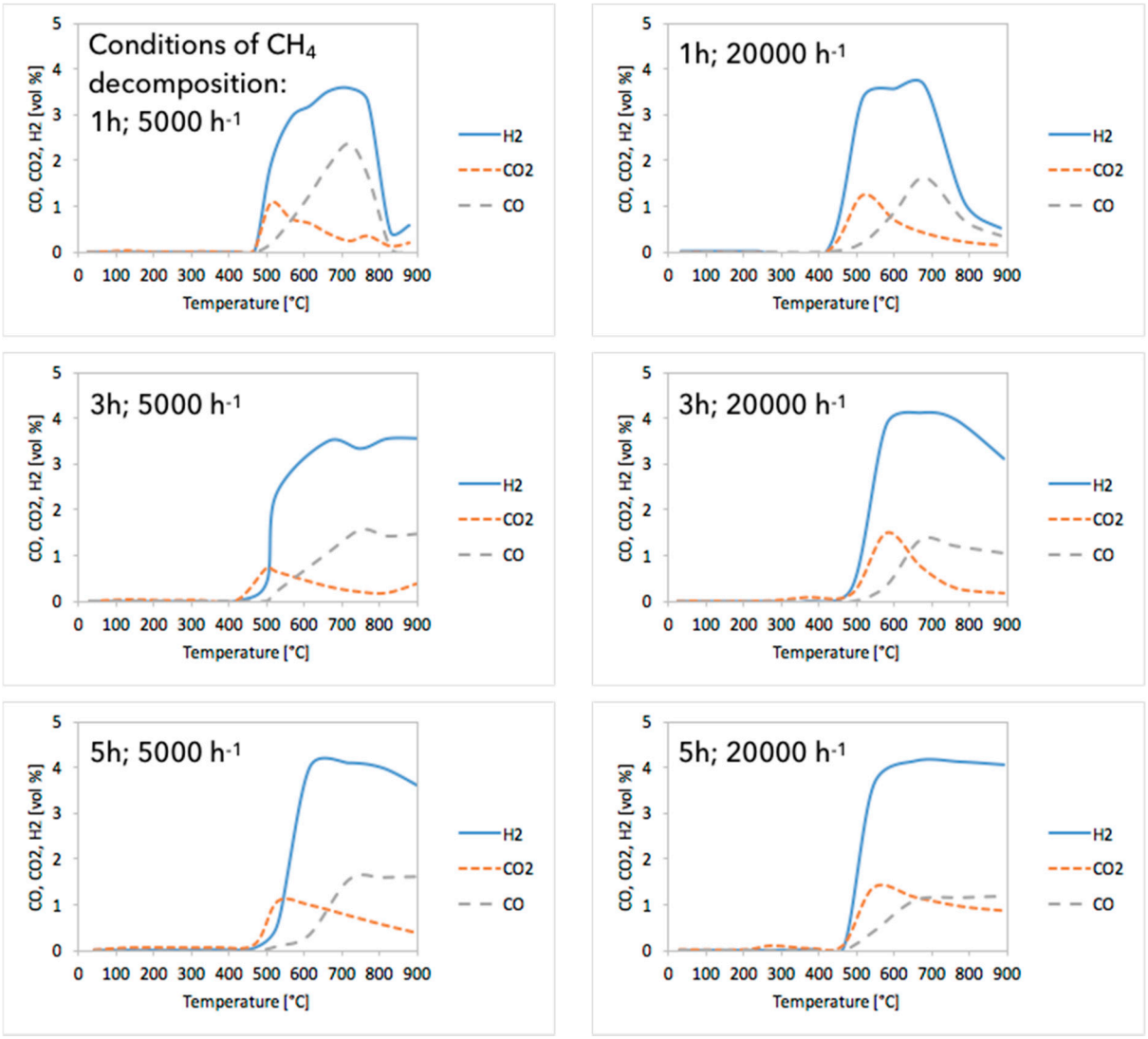

Figure S9. H_2, CO and CO_2 formation during regeneration of $Ni/CeZrO_2$ in 4.15 vol.% H_2O/Ar after 1, 3 and 5 hours of CH_4 deposition at 700 °C and GHSV of 5000 and 20,000 h^{-1}.

In each case small amounts of H_2 are observed from ca. 400 °C, while at 500–550 °C H_2O conversion usually exceeds 90%. The H_2O dissociates on catalyst active sites (*) being oxygen vacancies in $CeZrO_2$ or Ni^0 (Equation (S1)). Hydrogen desorbs from catalyst surface whereas oxygen (O*) that is still adsorbed on the active site can oxidize nearby carbon deposit to CO_2 (at lower temperatures) and to CO (at higher temperatures) (Equations (S2)–(S4)). Amorphous carbon deposits are oxidized at lower temperatures and structural carbon (CNTs) are oxidized at higher temperatures. According to TGA of catalyst samples after separation of deposit, the amorphous carbon prevailed.

$$H_2O + * = O^* + H_2 \quad (S1)$$

$$C + O^* = CO^* \quad (S2)$$

$$CO^* = CO + * \quad (S3)$$

$$CO + O^* = CO_2 + * \quad (S4)$$

$$C + 2H_2O = CO_2 + 2H_2 \quad (S5)$$

$$C + H_2O = CO + H_2 \quad (S6)$$

Rapid decrease in H_2 formation in the case of samples obtained after CH_4 decomposition for 1 hour is due to lower amount of carbon deposits on their surface. The rate of carbon deposits oxidation

is determined by temperature, whereas the duration of regeneration is determined by the amount of deposits on catalyst surface.

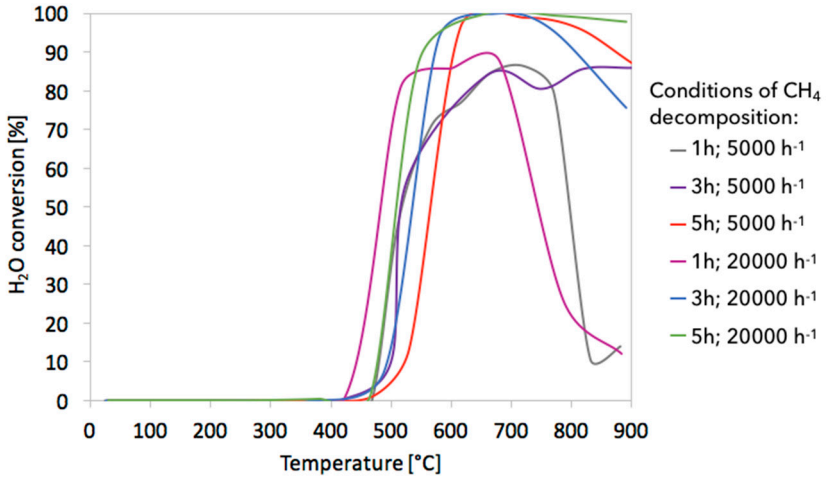

Figure S10. H_2O to H_2 conversion during regeneration of $Ni/CeZrO_2$ after 1, 3 and 5 hours of CH_4 deposition at 700 °C and GHSV of 5000 and 20,000 h^{-1}.

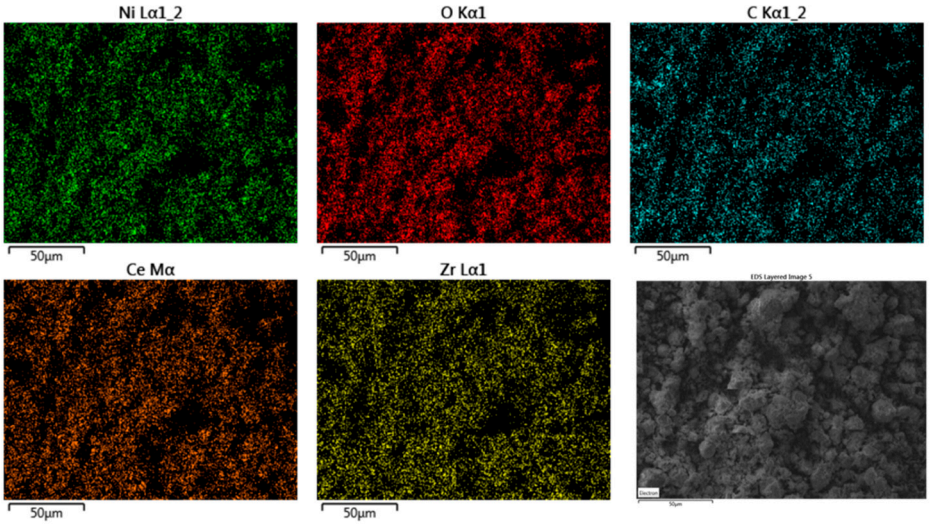

Figure S11. Ni, O, Ce, Zr and C mapping for $Ni/CeZrO_2$ after its 34-hour regeneration in 4.15 vol.% H_2O/Ar.

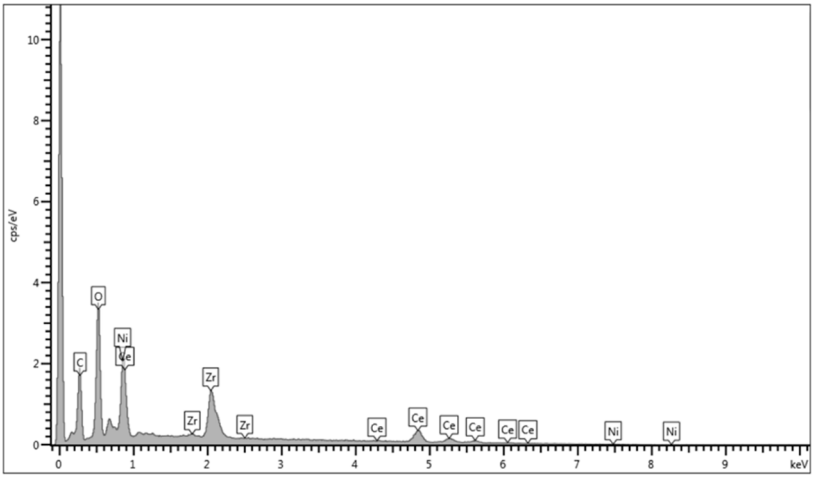

Figure S12. EDS for Ni/CeZrO$_2$ after 34-hour regeneration in 4.15 vol.% H$_2$O/Ar.

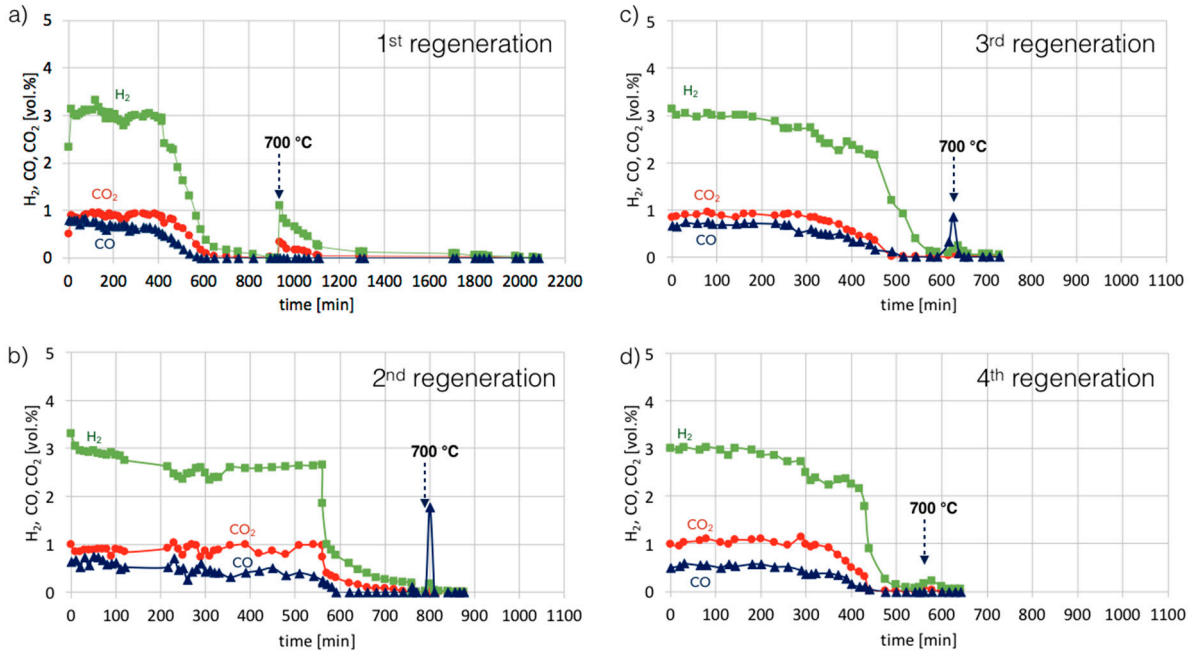

Figure S13. Composition of the gas on reactor outlet during subsequent regeneration tests of Ni/CeZrO$_2$ (4.15 vol.% H$_2$O/Ar, T = 550 and 700 °C, GHSV = 2000 h^{-1}).